LAWRENCE
LIVERMORE
NATIONAL
LABORATORY

UCRL-JRNL-227533

Molecular Dynamics Investigation of Adhesion between TATB Surfaces and Amorphous Fluoropolymers

R. H. Gee, A. Maiti, S. Bastea, L. Fried

January 29, 2007

Macromolecules

Molecular Dynamics Investigation of Adhesion between TATB Surfaces and Amorphous Fluoropolymers

Richard H. Gee*, Amitesh Maiti, Sorin Bastea and Laurence E. Fried

University of California
Lawrence Livermore National Laboratory
Chemistry, Materials, and Life Science Directorate
P.O. Box 808, L-268
Livermore, CA 94551

Abstract

Atomistic simulations are used to study the adhesion properties of amorphous perfluoro- and fluoro- polymers onto two different crystal surfaces of 1,3,5-triamino-2,4,6-trinitrobenzene (TATB). Properties of the bulk amorphous polymer melts are also investigated. The fluoropolymers studied in this article include Kel-F 800, Teflon® AF, Hyflon AD®, and Cytop®. Simulations of the bulk polymer melts were performed over a wide range of temperatures including the volumetric glass transition temperature, so as to validate the interaction parameters used. The computed glass transition temperatures and densities compare well with experiment. The solubility parameters for the various polymers also compare well with calculations based on group additive methods. The local molecular structure at the TATB interface, as well as the degree of adhesion varies from one polymer to another. All polymers except Hyflon show a propensity to readily wet the two TATB surfaces studied.

Keywords: Atomistic computer simulations; amorphous fluoropolymers; interfacial tension; plastic bonded explosives.

I. Introduction

* To whom correspondence should be addressed, e-mail: gee10@llnl.gov.

Fluoropolymers have many interesting properties not found in their hydrocarbon analogues.[1] These properties include low surface tension and coefficient of friction, novel piezoelectric and pyroelectric properties, low refractive index, and high chemical and thermal stabilities. Many fluoropolymers also demonstrate an unusually high density, high chemical stability, and mechanical properties suitable for use in the manufacture of pressed powder composites.[2] Furthermore, recently developed amorphous perfluorinated polymers have received increasing attention due to improved creep and adhesive properties.[3-5] Such properties make these polymers ideal candidates for use as binder materials in energetic material formulations, known as plastic-bonded explosives (PBX). Typical PBX formulations have five to ten percent polymer binder, which is assumed to coat the remaining solid energetic material particles.[6] Thus, good adhesion to the crystalline energetic material is of fundamental importance in providing safe, low-sensitivity PBX formulations.

Relatively few theoretical studies of the adhesion properties of PBXs have been reported in the literature. To this end, we investigate the adhesion of various fluoropolymers to two different crystal surfaces of the energetic material 1,3,5-triamino-2,4,6-trinitrobenzene (TATB) using molecular dynamic simulations (MD). Computer simulations have played an important role in investigating specific interactions between molecules.[7-13] Such studies are of obvious importance in determining the degree of adhesion, which has traditionally been difficult to address via experiment.

In this paper four different fluoropolymers melts are studied: Teflon® AF 1600 (AF), Cytop® (Cytop), Hyflon® AD 60 (Hyflon), and Kel-F 800 (Kel-F), where

abbreviated names are in parentheses. These polymers are simulated in contact with two different TATB crystal surfaces: [100], and [001].

II. Computational Method

a. The Polymer Representation and Amorphous cells

The MD simulations of the various fluoropolymers were carried out on a variety of bulk amorphous ensembles, as well as ensembles in which amorphous films of each of the four separate fluoropolymers are interfaced to either a [001] or a [100] surface of a TATB crystal.

The bulk amorphous simulations were performed on ensembles consisting of fifteen chains composed of 120 total monomer units per chain, for each of the four fluoropolymers studied. The Cytop fluoropolymer chains used in the simulations are composed of monomers shown in Fig. 1*a*. The remaining three fluoropolymers are copolymers. Teflon® AF 1600 copolymer chains were obtained by the simulated copolymerization of tetrafluoroethylene (TFE) monomer (35 % mole fraction) and 2,2-bistrifluoromethyl-4,5-difluoro-1,3-dioxole monomer (65 % mole fraction) (Fig. 1*b*); Hyflon AD 60 copolymer chains were obtained by the simulated copolymerization of TFE monomer (40 % mole fraction) and 2,2,4-trifluoro-5 trifluoromethoxy-1,3 dioxole monomer (60 % mole fraction) (Fig. 1*c*); and Kel-F 800 copolymer chains were obtained by the simulated copolymerization of chlorotrifluoroethylene and vinylidene fluoride monomers in a 3:1 mole ratio, respectively (Fig. 1*d*).

The initial starting polymer configurations for simulations in the bulk were generated using a Monte Carlo method.[14] The AF, Cytop, and Hyflon monomers were allowed to 'polymerize' in a head-to-tail manner with no monomer reversals, resulting in

the mole ratios referred to above, while the KelF monomers were allowed to 'polymerize' according to the procedure described in Ref. [15]. Additionally, each of the fifteen polymer chains was polymerized independently, thus providing a greater statistical representation of the bulk melts. The initial atomic positions of the amorphous melt structures were generated using a random distribution of torsional angles, which was generated using a Monte Carlo method that assigns random values to all rotatable torsions in the polymer chain. The resulting amorphous structure was then relaxed by energy minimization. Bulk simulations were carried out using cubic periodic boundary conditions. All atoms in the polymer chains were treated explicitly.

***b*. TATB Interfaces**

Each of the four fluoropolymers was interfaced to either a [001] or a [100] TATB surface.[16] The TATB surfaces were constructed by first creating an orthogonal bulk supercell from the experimental TATB unit cell and then placing a vacuum normal to the defined surface. We used a bulk supercell of dimensions a = 54.1386 Å, b = 46.8570 Å, and c = 43.9561 Å, consisting of 504 TATB molecules (12,096 total atoms). All TATB molecules were held fixed in the simulations. For all fluoropolymer / TATB interface simulations, the cell dimension normal to the [001] or [100] TATB interface was extended such that the density of the fluoropolymer at the TATB surface was equal to the equilibrium bulk density at 500 K,[17] as determined from the simulations of the bulk amorphous fluoropolymer melts; the remaining two axis dimensions were fixed (a = 54.1386 Å and b = 46.8570 Å for the [001] TATB interface; b = 46.8570 Å and c = 43.9561 Å for the [100] TATB interface). Each of the four different equilibrated amorphous polymer melts (equilibrated at 500 K), were place at either of the [001] or

[100] TATB surfaces, so as to render a melt phase consisting of fifteen polymer chains, adjacent to the TATB surface of interest. The ensembles thus created were allowed to equilibrate via *NVT* dynamics for a minimum of 2 *ns*. A data collection period of a minimum of 2 *ns*, and up to greater than 10 *ns* was used. The orthorhombic cell dimensions of the [001] TATB interface for AF, Cytop, Hyflon, and KelF, were c = 182.9 Å, 137.64 Å, 148.822 Å, and 190.0 Å, respectively. The orthorhombic cell dimensions of the [100] TATB interface for AF, Cytop, Hyflon, and KelF, were a = 225.185 Å, 169.528 Å, 183.296 Å, and 233.028 Å, respectively.

***c*. Potential Functions**

The MD simulations of the amorphous bulk fluoropolymer melts employed the COMPASS[18] force field parameter set. The COMPASS potential consists of valence terms including diagonal and off diagonal coupling terms, and non-bonded van der Waals (vdW) and Coulombic interaction terms. The functional form of the potential employs a quartic polynomial for bond stretching and angle bending and a three-term Fourier expansion for torsions. The atomic charges for the non-bonded Coulombic interaction are those parameterized by Sun *et al*.[18] The vdW interactions are implemented using the well-known Lennard-Jones (LJ) potential, and makes use of an inverse 9th-power term for the repulsive part rather than the more customary 12th-power term. All valence degrees of freedom were explicitly treated and unconstrained.

The interaction potentials used to treat the explicit crystalline TATB employed our recently developed force field parameter set[8], except that the vdW interactions were implemented using the LJ-9-6 potential. Further, all unlike atom pairs were determined using the 6th order combination law.[19]

d. Molecular Dynamics Method

The simulations of all bulk amorphous polymer melts were carried out using constant particle number, pressure, and temperature (*NPT)* dynamics at a pressure of 1 atm, using three-dimensional periodic boundary conditions. Simulations of the polymer/TATB interfaces were performed at a temperature of 500 K[17] using constant particle number, volume, and temperature (*NVT)* dynamics. All computations were carried out using the LAMMPS code.[20] The equations of motion were integrated using the Verlet algorithm[21] with a time step of 1.0 *fs.* A Nosé-Hoover thermostat[22] with a relaxation time of 0.1 *ps* was used to control the temperature, and the pressure was controlled isotropically.[23] The nonbonded vdW interactions were treated by truncating atom pairs with an inter-atomic distance greater than 20 Å, coupled with a long-range tail correction.[24] The particle-particle particle-mesh Ewald (PPPM) method[25] was used for the long-range treatment of electrostatic interactions.

The initial amorphous polymer melt was constructed to be of density ~1.0 g/cm^3. The lower-density initial state was found to improve the convergence of the equilibration procedure by avoiding close-contact high-energy configurations. All amorphous structures were initially simulated at 550 K under *NPT* conditions. The volume equilibration process was carried out for a minimum duration of 5 *ns*. Following this step, the systems were cooled in *NPT* runs in increments of 25 K or 50 K and equilibrated for 5 *ns* each at the desired temperature.

III. Simulation Results and Discussion

a. Amorphous cells and force-field validation

The computation of the volume-temperature (V-T) properties of amorphous AF, obtained from our MD simulations, is shown in Fig. 2 for the fifteen 120-mer chain melt. The V-T results are important for two reasons; first, the results, when compared to experimental data, provide a means of determining the quality of the force field parameters used in the simulations, and second, it allows for a direct prediction of the volumetric glass transition temperature, T_g, which is of fundamental importance in determining the material properties of the polymer. The V-T curve which shows a distinct break characteristic of vitrification, represents the location of the glass transition temperature. The extraction of the volumetric T_g in this manner is common, although only empirically justified.[15, 26-35] The simulation results reveal a T_g which occurs at ~162 ^{o}C, as compared to the experimentally determined T_g of 160 ^{o}C K,[36] while, the calculated volumetric coefficient of thermal expansion, $\beta = V_o^{-1}\left[\frac{\delta V}{\delta T}\right]_p$, above and below T_g are ~1039 ppm/^{o}C and ~255 ppm/^{o}C, respectively, as compared to the experimental values of 960 ppm/^{o}C and 222 ppm/^{o}C, respectively. Thus, the simulations results are in excellent agreement with experiment, and demonstrates the accuracy of the COMPASS[18] force field parameter set used here. Table 1 summarizes our simulation results for all four polymers and compare with room-temperature experimental results, where available. The computed glass transition temperatures and densities, for the various fluoropolymers compare well to experiment.

As a further check to the validity of the interaction potentials used here, Table 1 compares the solubility parameters, δ, predicted using the van Krevelen group additive method[37] for the four different fluoropolymers studied here at 300 K, to our computed

solubility parameters, where $\delta = \sqrt{\Delta E/V}$, and V is the molar volume, and ΔE is the nonbonded potential energy difference between the bulk melt state and that in which the macromolecules can no longer feel each other. The computed solubility parameters for the various fluoropolymers compare well to that predicted by the van Krevelen group additive method.[37] Accurate values for the computed solubility parameter is essential, since the polymer cohesive energy directly affect the overall wetting behavior of the polymer when interfaced to a solid substrate.

***b*. Interfaces and Surface Properties**

As mentioned in Section II.*b*, the TATB/fluoropolymer interfaces were constructed by bringing the amorphous fluoropolymer melts close to the TATB interface. An example of such an ensemble is given in Fig. 3 for Cytop interfaced to the [001] TATB surface. The potential energy of the interface structures were minimized using MM energy minimization techniques and then subjecting to a minimum of 5 *ns* MD simulations at ~500 K, during which, various interfacial properties were monitored.

Of particular interest here is the study of the surface properties, namely, the interfacial tension, γ_{12} , work of adhesion, W_{12} , and spreading coefficient, *S*. The corresponding microscopic expression for the interfacial tension for the [001] and [100] TATB/polymer interfaces, written in terms of the pressure tensor[38-40] is,

$$\gamma_{12}^{[001]} = \frac{L_z}{2}\left[p_{zz} - \tfrac{1}{2}\left(p_{xx} + p_{yy}\right)\right] , \qquad (1)$$

$$\gamma_{12}^{[100]} = \frac{L_x}{2}\left[p_{xx} - \tfrac{1}{2}\left(p_{yy} + p_{zz}\right)\right] , \qquad (2)$$

where $p_{\alpha\alpha}$ ($\alpha = x, y, or\ z$) is the $\alpha\alpha$ element of the pressure tensor and L_z and L_x are the lengths of the simulation cell in the *z* and *x* directions, respectively. The work of

adhesion, W_{12}, is calculated as the difference between the TATB surface tensions, γ_1, the fluoropolymer surface tensions, γ_2, and the interfacial tension, γ_{12}, as

$$W_{12} = \gamma_1 + \gamma_2 - \gamma_{12}. \quad (3)$$

The TATB surface tensions, γ_1, for the [001] and [100] surface were computed as the difference in energy between the interfacial structure ($E_{\text{interface}}$) and the TATB bulk energy, E_{bulk} as,

$$\gamma_1 = \frac{\left(E_{\text{interface}} - E_{\text{bulk}}\right)}{2A}, \quad (4)$$

where the surface area is $2A$, as two surfaces of area, A, are formed upon the creation of the interface. The various fluoropolymer surface tensions, γ_2, used to compute W_{12}, where obtained from the molar parachors.[37]

Finally, the spreading coefficient, S, is defined as

$$S = \gamma_1 - \gamma_2 - \gamma_{12}. \quad (5)$$

With this definition, positive values of S indicate that the liquid polymer will spread onto the solid surface, while negative values imply that the liquid polymer will contract, and a value of zero means the liquid has no propensity to wet the solid surface. Table 2 shows the values for the computed surface tensions, interfacial tensions, work of adhesion, and spreading coefficients for the four fluoropolymers at each of the two TATB surface. The computed work for the adhesion, W_{12}, and interfacial tension, γ_{12} show a distinct difference between the two TATB surfaces. The interfacial tension for the [001] TATB surface, $\gamma_{12}^{[001]}$, is positive for all polymers, whereas the interfacial tension the [100] surface, $\gamma_{12}^{[100]}$, are all significantly negative. This is also borne out in the computed W_{12}

values, where a decrease of the interfacial energy leads to an increase in W_{12}, which are all found to be substantially greater at the [100] TATB surface.

The difference in the interfacial tension between the two TATB surfaces may be attributed to the roughly ~45 % increase in the available accessible surface area of the [100] TATB surface as compared to the [001] TATB surface (based on a Connolly surface construction[41, 42]) for which the polymer can bind. Furthermore, the pendent –NH_2 and –NO_2 moieties of TATB which are exposed at the [100] surface, may play a role in the overall adhesion properties due to the presence of the dipole-dipole interactions between the –NH_2 and –NO_2 moieties and the polymer. The rough [100] TATB surface is shown in Fig. 4, along with the Connolly accessible surface. To illustrate this point, Fig. 5 shows a single Cytop polymer chain geometry after ~0.3 *ns NVT* dynamics following the introduction of the chain to the TATB surface (Fig. 5*a* shows the geometry at the [001] TATB surface; Fig. 5*b* shows the geometry at the [100] TATB surface). As is apparent, the polymer chain at the [100] TATB surface migrates into the rough "cavities" along the surface, in contrast to the relatively "flat" geometry seen along the [001] TATB surface.

The polymers' ability to wet the solid TATB surface is reflected in the computed spreading coefficient, *S.* As seen in Table 2, the computed spreading coefficient, and thus, the ability to wet the solid TATB surface, for all polymers, is significantly greater at the [100] TATB surface as compared to the [001] TATB surface. In fact, the computed negative value of the spreading coefficient for Hyflon at the [001] TATB surface suggests that Hyflon does not wet the [001] TATB surface. The weak adhesion seen for Hyflon at the [001] TATB surface could be due in part to the bulky pendent –O-CF_3

moiety (see Fig. 1*c*), which effectively inhibits efficient surface packing at the smooth [001] TATB surface.

To further illustrate the diminished wetting of the Hyflon polymer as compared to the other polymers studied here, we monitor the time averaged density profile of the polymers at both the [001] and [100] TATB surfaces. Fig. 6*a* shows the density variation of the pendent fluorine atoms as a function of interfacial distance from the [001] TATB surface for all polymers studied here. It is found, that the fluorine density profile for the Hyflon polymer is relatively structureless, as compared to the other polymers. In contrast, all polymers, except Hyflon, show two distinct peaks close to the [001] TATB interface. The lack of apparent structure of the Hyflon polymer further illustrates the diminished wetting of the Hyflon polymer as compared to the others studied here. Fig 6*b* shows the time averaged density profiles for all moieties present in the Cytop polymer for comparison purposes.

As a qualitative measure of the enhanced spreading at the [100] TATB surface as compared to the [001] TATB surface, as single 120-mer Cytop polymer chain was allowed to dynamically evolve for 0.3 *ns* on each of the [001] and [100] TATB surfaces in 2-dimensional MD simulations). The TATB surface consisted of 4,536 TATB molecules (108,864 total TATB atoms) with [001] and [100] TATB surface dimensions of a = 169.528 Å X b = 140.571 Å and b = 140.571 Å X c = 131.868 Å, respectively. Fig. 7 & 8 shows the time evolution of the single Cytop 120-mer polymer chain at the [001] and [100] TATB surface, respectively. It is apparent that the single Cytop polymer chain readily spreads onto both the [001] and [100] TATB surface. Qualitatively however, the

polymer at the [100] TATB interface seems to spread more evenly, and readily penetrate into the rough [100] TATB cavities.

IV. Conclusion

The focus of this article is on the adhesion properties of fluoro- and perfluoro-polymers onto TATB crystal surfaces. To our knowledge, this is the first instance of such a study concerning the novel Cytop, Hyflon, and AF amorphous perfluoropolymers. It was determined that the COMPASS[18] force field used here accurately predicted the volume-temperature behavior of this novel class of polymers., It was found that all polymers studied here except Hyflon have a propensity to readily wet the two TATB surfaces studied. Hyflon wets only the TATB [100] surface. Further, the adhesion onto the [100] TATB surface is significantly favored over adhesion onto the [001] TATB surface mainly due to the increase in the accessible surface area in the former. The current study could be helpful in determining polymeric binders suitable for use with TATB.

Acknowledgements

The work was performed under the auspices of the U.S. Department of Energy by the University of California Lawrence Livermore National Laboratory under Contract W-7405-Eng-48.

Table 1. Glass transition temperatures, densities, and solubility parameters of various fluoropolymers and TATB.

	T_g (°C)		ρ (g/cm^3) @ 298 K			δ (J/cm^3)$^{1/2}$ @ 298 K	
	Exp	MD	Exp	MD	Synthia	MD	van Krevelen**
Kel-F 800	22-34	18	2.00	1.91	1.93	16.1 [14.8-16.2]*	16.3
Cytop	108	110	2.03	1.96	2.085	12.8	13.2
Hyflon AD 60	110-121	115	1.93	1.97	2.047	13.3	14.4
AF 1600	160	160	1.814	1.86	2.065	13.9	13.8
TATB	---	---	1.937	1.938	---		---

*Experimental range for poly(chlorotrifluoroethylene) (Cady *et al.)*.

**Ref. [37].

$\delta = \sqrt{\Delta E/V}$, where V is the molar volume, and ΔE is the nonbonded potential energy difference between the bulk melt state and that in which the macromolecules can no longer feel each other.

Table 2. Summary of surface tension, γ, work of adhesion, W_{12}, and interfacial tension, γ_{12}, and spreading coefficient, S, for various fluoropolymers (γ_2) interfaced to TATB (γ_1) in (erg cm^{-2}).

Interface [001]	γ_1	γ_2^{MP}	W_{12}	γ_{12}	S
KelF	+66	+27	+76	+17 ± 1	+22
Cytop	+66	+24	+87	+3 ± 2	+39
AF	+66	+23	+78	+11 ± 1	+37
Hyflon	+66	+22	+5	+83 ± 2	-39
Interface [100]	γ_1	γ_2^{MP}	W_{12}	γ_{12}	S
KelF	+208	+27	+271	-36 ± 2	+217
Cytop	+208	+24	+275	-43 ± 1	+227
AF	+208	+23	+281	-50 ± 1	+235
Hyflon	+208	+22	+320	-90 ± 1	+276

γ_2^{MP} ≡ surface tension determined from the molar parachor group additive method at 500 K.

FIGURES

Figure 1: Monomer chemical structures of Cytop (a), Teflon AF (b), Hyflon AD (c), and Kel-F 800 (d).

Figure 2: Specific volume versus temperature for AF at 1 atm as determined from *NPT* dynamics. MD results are shown by open symbols (circles); experimental values for T_g (solid diamond) and experimentally determined coefficient of thermal expansion (solid lines) are also shown.[36]

Figure 3: Typical [001] TATB / polymer interface used in the MD simulations.

Figure 4: Illustration of the topologically rough [100] TATB Connolly surface, normal to the interfacial surface (a), and perpendicular to the interface (b).

Figure 5: Snapshot of a single Cytop polymer chain geometry at the [001] and [100] TATB surfaces (a and b, respectively) after ~300 *ps* at 211 K above the polymers T_g. The increased surface area available to the polymer on the [100] TATB surface is apparent.

Figure 6: Fluorine density profiles for all polymers studied here at the [001] TATB interface (in density units) at 500 K, (a). Panel (b) shows the density profiles for the carbon, fluorine, and oxygen atoms for Cytop polymer at the [001] TATB interface.

Figure 7: Snapshots of the time evolution of a single Cytop polymer chain at the [001] TATB interface at 60 *ps* intervals (label 1 = 0 *ps*; label 2 = 60 *ps*; label 3 = 120 *ps*; label 4 = 180 *ps*; label 5 = 240 *ps*; label 6 = 300 *ps*).

Figure 8: Snapshots of the time evolution of a single Cytop polymer chain at the [100] TATB interface at 60 *ps* intervals (label 1 = 0 *ps*; label 2 = 60 *ps*; label 3 = 120 *ps*; label 4 = 180 *ps*; label 5 = 240 *ps*; label 6 = 300 *ps*).

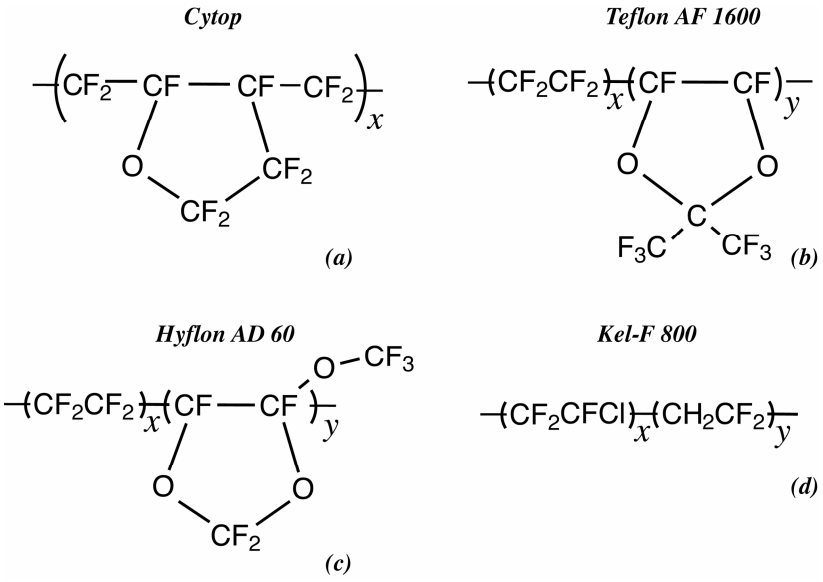

Figure 1. – R.H. Gee:

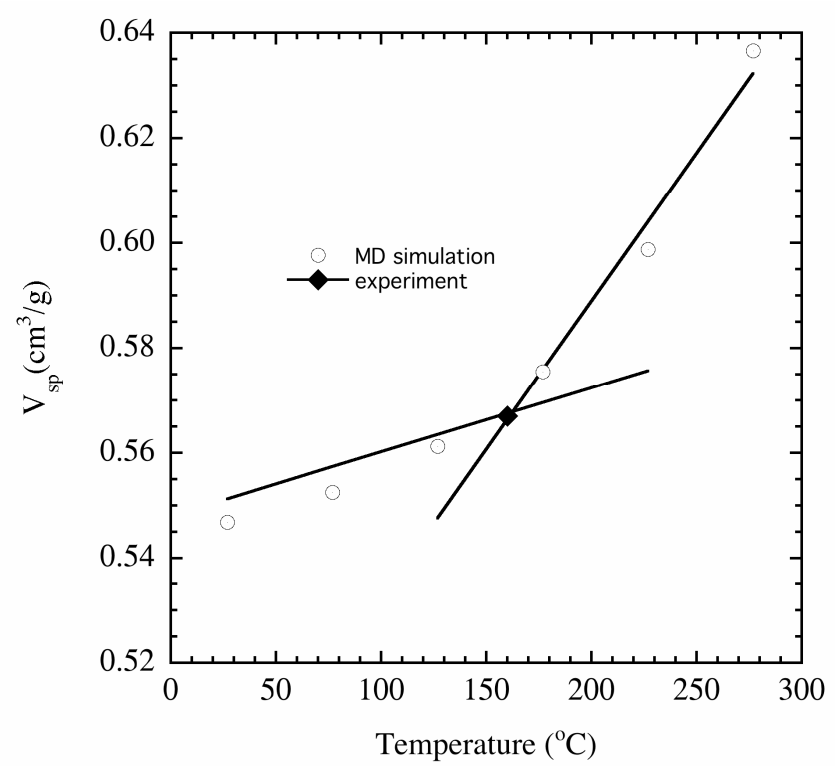

Figure 2. – R.H. Gee

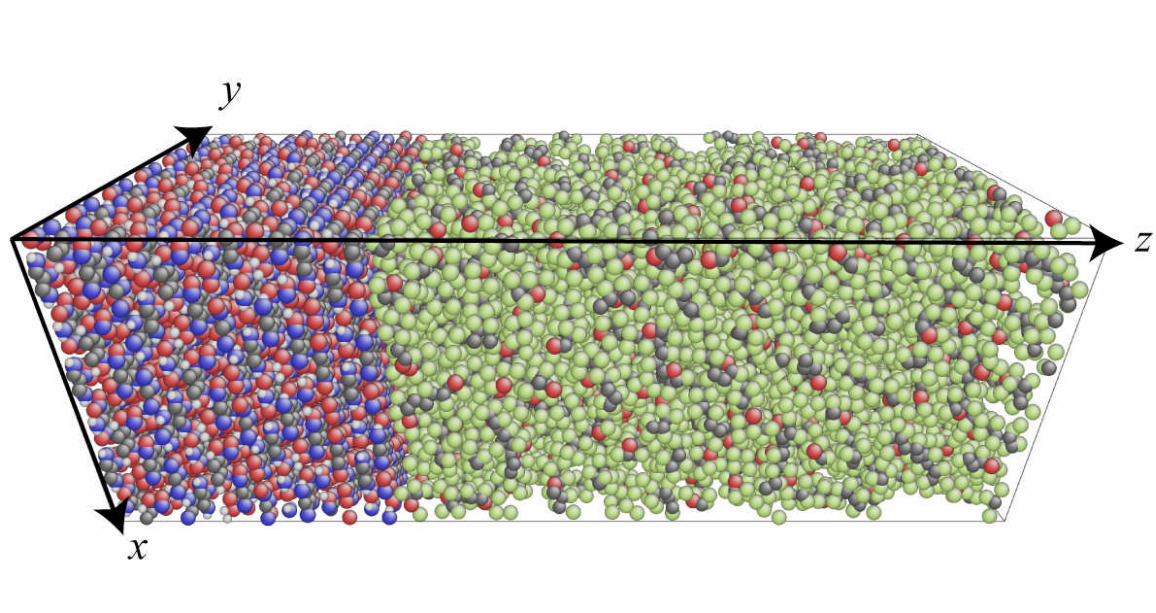

Figure 3. – R.H. Gee

(a)

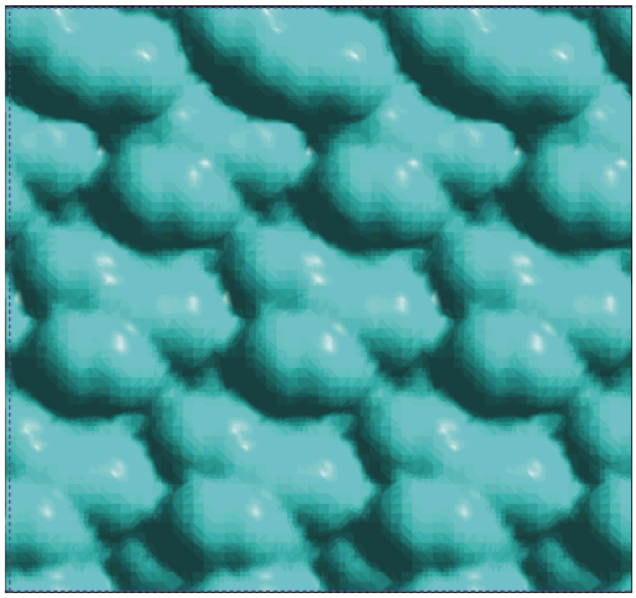

(b)

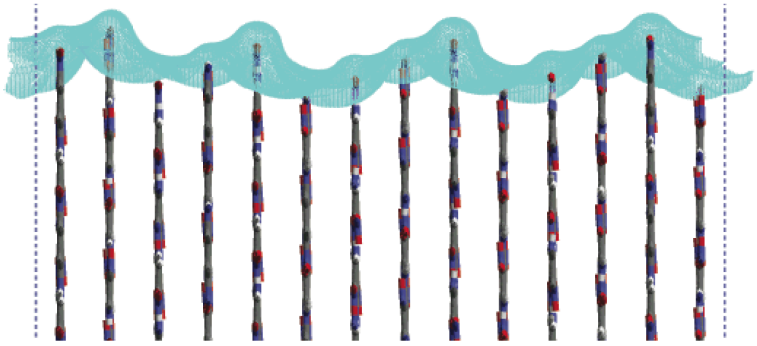

Figure 4. – R.H. Gee

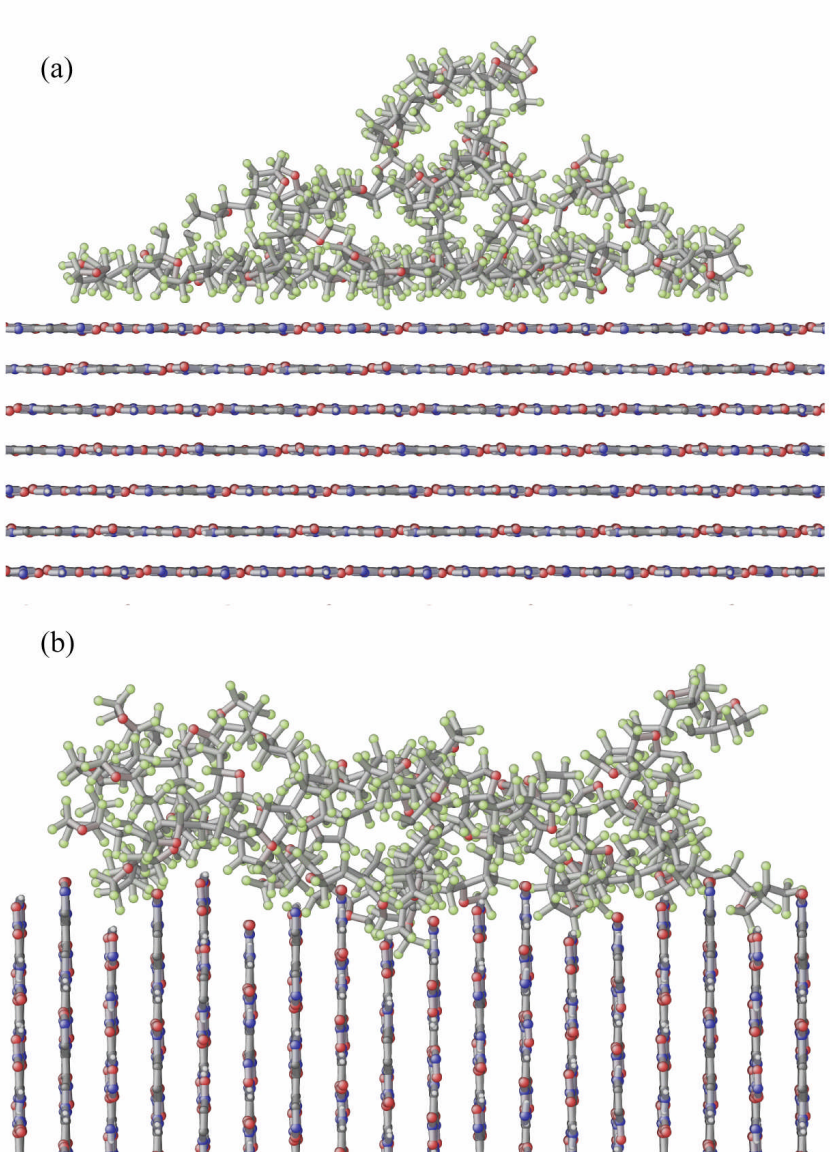

Figure 5. – R.H. Gee

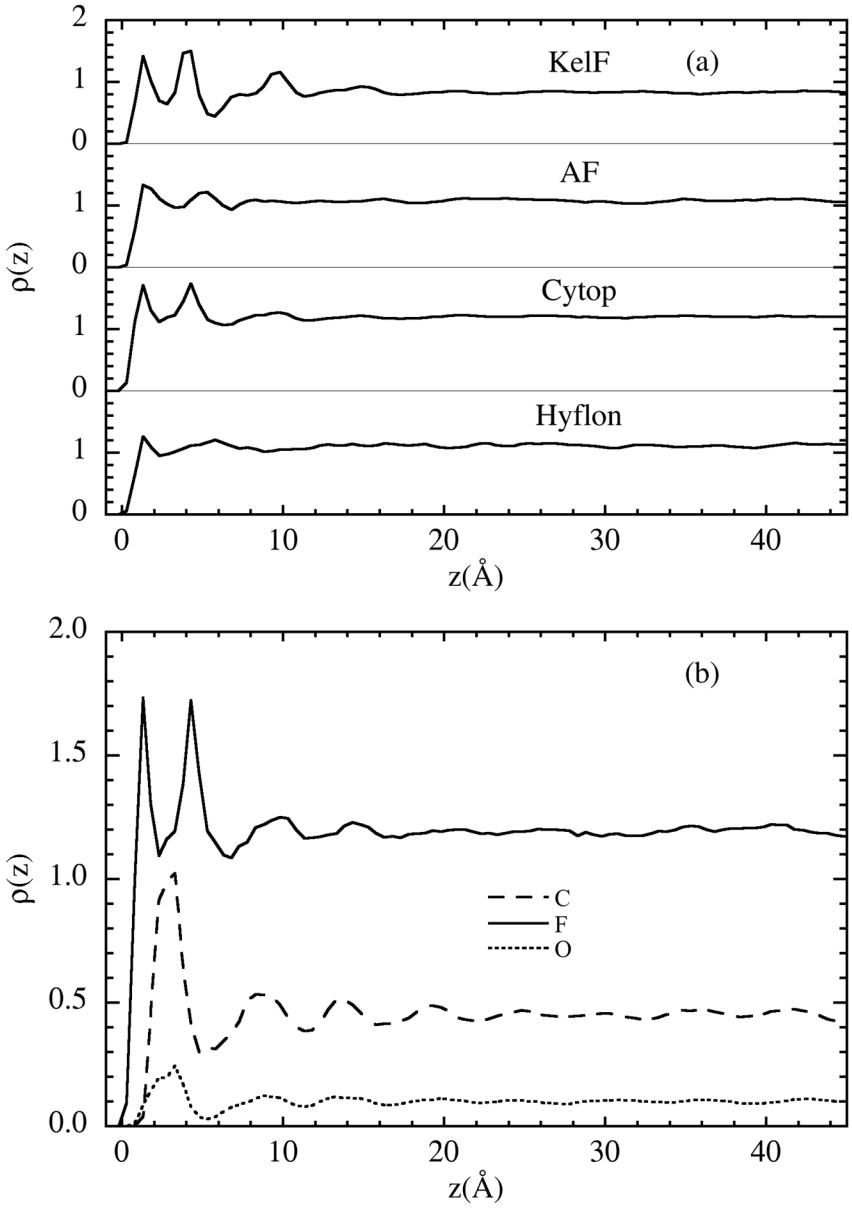

Figure 6. – R.H. Gee

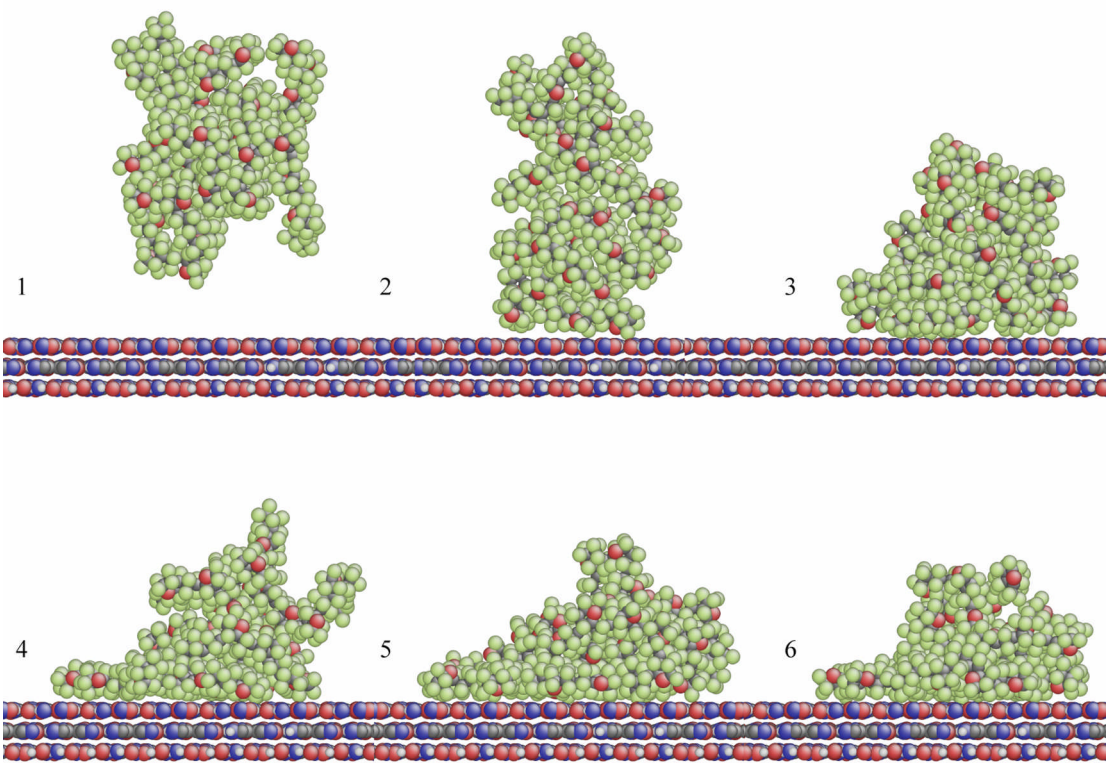

Figure 7. – R.H. Gee

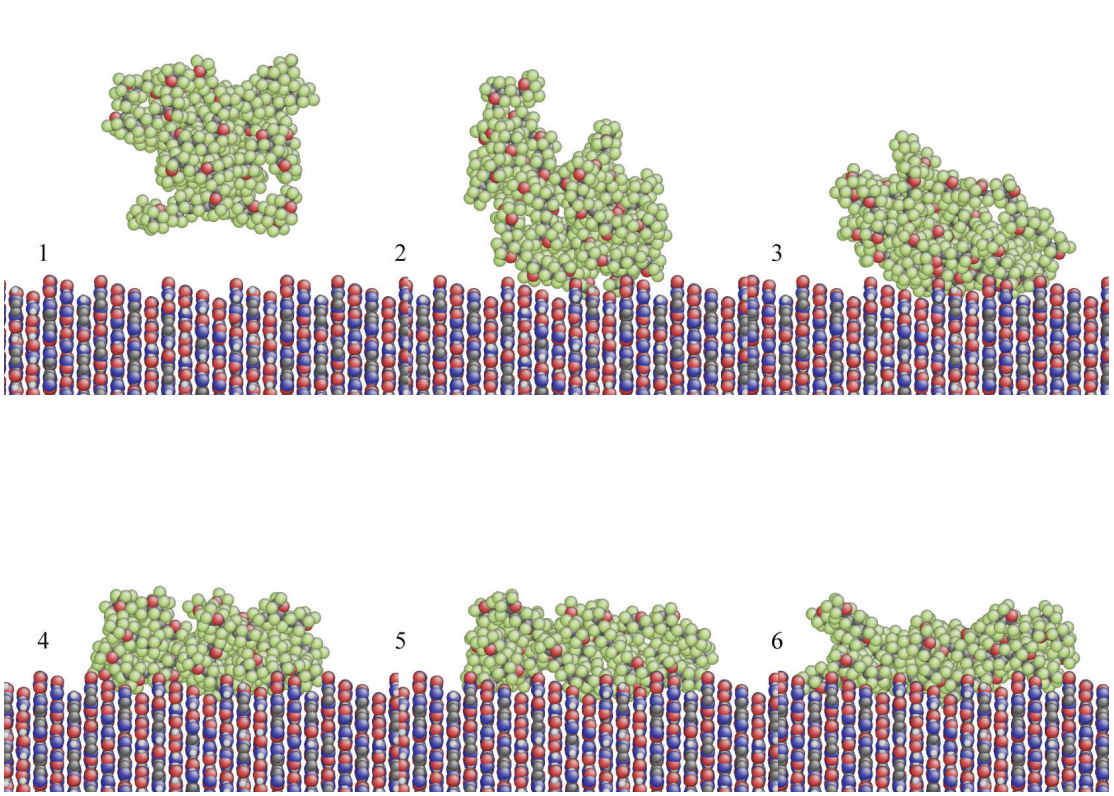

Figure 8. – R.H. Gee

References and Notes

1. Lovinger, A. J., Development in Crystalline Polymers. Applied Science, London: 1982; Vol. 1.

2. James, E. The Development of Plastic Bonded Explosives; UCRL-12439-T; Lawrence Livermore National Laboratory: Livermore, CA, 1965.

3. http://www.solvaysolexis.com/Resources.htm#HyflonPFA

4. A brochure detailing the technical properties of the Teflon AF 1600 product can be obtained from the Du Pont corporation, Wilmington, DE; No. HO7805.

5. Sugiyama, N., Modern Fluoropolymers: High Performance Polymers for Diverse Applications. John Wiley & Sons: 1997; p 541.

6. Pruneda, C. O.; Kolb, J. R.; Bower, J. K. I & EC Product Research and Development 1980, 19, 326.

7. Roszak, S.; Gee, R. H.; Balasubramanian, K.; Fried, L. E. Chemical Physics Letters 2003, 374, (3-4), 286-296.

8. Gee, R. H.; Roszak, S.; Balasubramanian, K.; Fried, L. E. Journal Of Chemical Physics 2004, 120, (15), 7059-7066.

9. Gee, R. H.; Maxwell, R. S.; Balazs, B. Polymer 2004, 45, (11), 3885-3891.

10. Goncharov, A. F.; Manaa, M. R.; Zaug, J. M.; Gee, R. H.; Fried, L. E.; Montgomery, W. B. Physical Review Letters 2005, 94, (6).

11. Roszak, S.; Gee, R. H.; Balasubramanian, K.; Fried, L. E. Journal Of Chemical Physics 2005, 123, (14).

12. Maiti, A.; Gee, R.; Maxwell, R.; Saab, A. Journal Of Physical Chemistry B 2006, 110, (8), 3499-3503.

13. Zepeda-Ruiz, L. A.; Maiti, A.; Gee, R.; Gilmer, G. H.; Weeks, B. L. Journal Of Crystal Growth 2006, 291, (2), 461-467.

14. Molecular Simulations, Inc.; San Diego, CA.: 1999.

15. Gee, R. H.; Fried, L. E.; Cook, R. C. Macromolecules 2001, 34, (9), 3050-3059.

16. The [001] and [100] TATB surfaces were chosen to be studied here, since they are two of the most prominently expressed TATB surfaces as determined from the Hartman-Perdok crystal growth morphology method [P. Hartman, W.G. Perdok, Acta Crystallogr. 8 49 (1955)].

17. The temperature was chosen so as to be above the glass transition temperatures for all the polymers considered here.

18. Sun, H. Journal of Physical Chemistry B 1998, 102, (38), 7338-7364.

19. Durig, J. R.; Sheehan, T. G. Raman Spectrosc. 1990, 21, 635.

20. Plimpton, S. J. J. Comp. Phys. 1995, 117, 1-19.

21. Verlet, L. Phys. Rev. 1967, 159, 98.

22. Nosé, S. J. Chem. Phys. 1984, 81, 511.

23. Melchionna, S.; Ciccotti, G.; Holian, B. L. Mol. Phys. 1993, 78, 533.

24. Allen, M. P.; Tildesley, D. J., Computer Simulation of Liquids. Clarendon Press: Oxford, U.K.: 1989.

25. Hockney, R. W.; Eastwood, J. W., Computer Simulation using Particles. McGraw-Hill: New York, 1981.

26. Boyd, R. H.; Gee, R. H.; Han, J.; Jin, Y. Journal Of Chemical Physics 1994, 101, (1), 788-797.

27. Gee, R. H.; Boyd, R. H. Polymer 1995, 36, (7), 1435-1440.

28. Gee, R. H.; Boyd, R. H. Journal Of Chemical Physics 1994, 101, (9), 8028-8038.

29. Han, J.; Boyd, R. H. Macromolecules 1994, 27, 5365.

30. Han, J.; Boyd, R. H. Polymer 1996, 37, 1797.

31. Han, J.; Gee, R. H.; Boyd, R. H. Macromolecules 1994, 27, (26), 7781-7784.

32. Pant, P. V. K.; J., H.; Smith, G. D.; Boyd, R. H. J. Chem. Phys. 1993, 99, 597.

33. Rigby, D.; Roe, R.-J. J. Chem. Phys. 1988, 89, (8), 5280.

34. Boyd, R. H. Trends In Polymer Science 1996, 4, (1), 12-17.

35. Bharadwaj, R. K.; Berry, R. J.; Farmer, B. L. Polymer 2000, 41, (19), 7209-7221.

36. Resnick, P. R.; Buck, W. H., Modern Fluoropolymers: High Performance Polymers for Diverse Applications. John Wiley & Sons: New York, 1997; p 397.

37. Bicerano, J., Prediction of Polymer Properties. Third Edition ed.; Marcel Dekker, Inc.: New York, 2002.

38. Croxton, C. A., Statistical Mechanics of the Liquid Surface. John Wiley & Sons: Chichester, 1980.

39. Kirkwood, J. G.; Buff, F. P. J. Chem. Phys. 1949, 17, 338.

40. Rowlinson, J. S.; Widom, B., Molecular Theory of Capillarity. Clarendon: Oxford, 1982.

41. Connolly, M. L. Science 1983, 221, 709.

42. Connolly, M. L. J. Appl. Crystal. 1983, 16, 548.